

## Metavanadate at the Active Site of the Phosphatase VHZ

Vyacheslav I. Kuznetsov,<sup>†</sup> Anastassia N. Alexandrova,<sup>\*,‡</sup> and Alvan C. Hengge<sup>\*,†</sup>

<sup>†</sup>Department of Chemistry and Biochemistry, Utah State University, Logan, Utah 84322-0300, United States

<sup>‡</sup>Department of Chemistry and Biochemistry, University of California, Los Angeles, California 90095-1569, United States

**S** Supporting Information

**ABSTRACT:** Vanadate is a potent modulator of a number of biological processes and has been shown by crystal structures and NMR spectroscopy to interact with numerous enzymes. Although these effects often occur under conditions where oligomeric forms dominate, the crystal structures and NMR data suggest that the inhibitory form is usually monomeric orthovanadate, a particularly good inhibitor of phosphatases because of its ability to form stable trigonal-bipyramidal complexes. We performed a computational analysis of a 1.14 Å structure of the phosphatase VHZ in complex with an unusual metavanadate species and compared it with two classical trigonal-bipyramidal vanadate–phosphatase complexes. The results support extensive delocalized bonding to the apical ligands in the classical structures. In contrast, in the VHZ metavanadate complex, the central, planar  $\text{VO}_3^-$  moiety has only one apical ligand, the nucleophilic Cys95, and a gap in electron density between V and S. A computational analysis showed that the V–S interaction is primarily ionic. A mechanism is proposed to explain the formation of metavanadate in the active site from a dimeric vanadate species that previous crystallographic evidence has shown to be able to bind to the active sites of phosphatases related to VHZ. Together, the results show that the interaction of vanadate with biological systems is not solely reliant upon the prior formation of a particular inhibitory form in solution. The catalytic properties of an enzyme may act upon the oligomeric forms primarily present in solution to generate species such as the metavanadate ion observed in the VHZ structure.

Because of vanadate's ability to modulate a number of biological processes, there is considerable interest in the origin of the interactions of this simple inorganic species with proteins.<sup>1</sup> Over 173 structures in the Protein Data Bank (PDB) display the interactions of different vanadate forms with a broad range of enzymes from multiple organisms.<sup>2</sup> Vanadate is a potent inhibitor of many phosphatases, enzymes with key roles in biological signaling throughout the living world. In particular, the insulin mimetic effect of vanadate is associated with its inhibition of protein tyrosine phosphatases (PTPs).<sup>3</sup> Compared with orthophosphate ion ( $\text{PO}_4^{3-}$ ), orthovanadate ion ( $\text{VO}_4^{3-}$ ) is a more potent inhibitor of phosphatases, with a  $K_i$  that is often several orders of magnitude lower. This difference is attributed to the ability of vanadate to form a trigonal-bipyramidal complex at the active site, resembling the transition state for phosphoryl transfer.<sup>2c,4</sup> Experimental data for PTPs indicate that both the

formation and hydrolysis of the phosphoenzyme intermediate proceed via a loose transition state with low bond orders to the nucleophile and the departing leaving group,<sup>5</sup> whereas crystal structures of trigonal-bipyramidal vanadate complexes in enzymes are commonly modeled with full bonds to the apical ligands. Previous experimental and computational results have suggested that such complexes resemble the transition state only in overall geometry and charge, whereas the bond orders between V and the apical ligands are higher than those of the corresponding bonds in the transition state.<sup>6</sup>

An understanding of the inhibitory effect of vanadate on phosphatases and its other biological effects is complicated by the tendency of vanadate to oligomerize in solution.<sup>7</sup> These effects are frequently observed under conditions where vanadate is primarily oligomerized and the monomer is a minor form.<sup>1c,7</sup> Interestingly, even though crystallization conditions often require vanadate concentrations that would primarily result in oligomeric species, crystal structures almost exclusively show monomeric vanadate in the active site. This has been attributed to the facile interconvertibility of different vanadate species in solution and the ability of the active site of phosphatases to stabilize the monomeric form selectively.<sup>8</sup> Here we report results indicating that the classical trigonal-bipyramidal vanadate species is not the only form capable of binding to PTPs and that other forms contribute to the inhibition of PTPs and potentially to other biological effects of vanadate.

VHZ is a recently described member of the PTP family of phosphatases.<sup>9</sup> The name VHZ denotes VH1-like member Z, one of the group of small *Vaccinia* virus VH1-related dual specific phosphatases. A recently obtained high-resolution structure of VHZ in complex with vanadate (PDB entry 4ERC) revealed what appeared to be an unusual "metavanadate" in the active site (Figure 1). The  $\text{VO}_3^-$  moiety is coordinated to the S atom of Cys95 as one apical ligand, with a V–S distance of 2.4 Å. The opposite apical position is occupied by a nitrogen atom of the Arg60 ( $\text{R}^{S60}$ ) side chain trapped in the active site from a symmetry-related VHZ molecule in the crystal (A in Figure 2). The V–N distance of 3.2 Å argues against a significant bonding interaction, and a significant interaction with the positively charged guanidinium group would not be expected. Although the V–S distance is typical of those commonly observed in trigonal-bipyramidal vanadate–PTP complexes,<sup>4b</sup> a distinct electron density gap between the atoms is evident in the high-resolution unbiased composite omit map (Figure 1). Furthermore, the  $\text{VO}_3^-$  moiety is nearly planar, while a tetrahedral geometry would

Received: June 8, 2012

Published: August 9, 2012

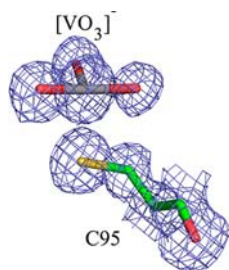


**Figure 1.** The electron density in the VHZ active site suggests a noncovalently bound  $\text{VO}_3^-$  ion. Shown is an unbiased composite omit map contoured at  $1.5\sigma$  in the refined model.

be expected for a covalent V–S bond in the absence of an apical V–N bond.<sup>4e,10</sup> These observations suggest that the  $\text{VO}_3^-$  moiety is better described as an electrostatically stabilized metavanadate ion ( $\text{VO}_3^-$ ) rather than a covalent thiovanadate adduct. A computational analysis was carried out to analyze the unusual bonding in this complex compared with more typical, previously reported vanadate–PTP structures (Figure 2). The two more conventional structures chosen for comparison were the complex of PTP1B with a vanadate ester of the peptide DADEYL (PDB entry 3I7Z; **B** in Figure 2) and the complex of PTP1B with orthovanadate (PDB entry 3I80; **C** in Figure 2). Both of the latter structures are typical of the trigonal-bipyramidal vanadate–PTP complexes that are well-represented in the literature. The nature of the chemical bonding between the  $\text{VO}_3^-$  ion and the protein was assessed using quantum-mechanical calculations. For this purpose, the portions of the proteins shown in Figure 2 were extracted directly from the crystal structures.

Truncation was done to include all residues that interact with vanadate; all residues with hydrogen-bonding or  $\pi$ -stacking interactions with residues that interact with vanadate; and all groups that are polar or charged and located in proximity to the vanadate ion, even if they do not directly interact. Hydrogen atoms were added to satisfy all dangling valencies using the Chimera program.<sup>11</sup> The standard protonation states of amino acids were assumed (deprotonated Asp and Glu, protonated Lys and Arg), except for the Tyr that coordinates V in **B**, which was deprotonated. The nucleophilic cysteine was assumed to be deprotonated; this residue has a  $\text{p}K_a$  of 5.5–6 in this enzyme family.<sup>12</sup> The truncated complexes effectively contained the first and second coordination spheres of the vanadate ion and consisted of 140–170 atoms (including hydrogens) depending

on the complex. The spin states of the complexes were zero, assuming the d subshell in V to be empty. Natural bond orbital (NBO) analysis<sup>13</sup> at the B3LYP<sup>14</sup>/6-31G\*<sup>15</sup> level of theory was used to elucidate the chemical bonds present in the complexes. This level of approximation, including the fairly modest size of the basis set, was considered adequate for the problem at hand because NBO results in general are quite insensitive to the basis set used and because only a qualitative assessment was needed to differentiate the states of V in the complexes. Calculations were performed using the Gaussian 09 suite of programs.<sup>16</sup>

Table 1 contains the key electronic structure parameters characterizing the V atom and its bonding environment in the

**Table 1. Electronic Structure Parameters Characterizing the V Atom and Its Bonding in Complexes A–C Shown in Figure 2, Calculated with NBO at the B3LYP/6-31G\* Level: Atomic Charges ( $Q$ ) and Electronic Populations of  $2c-2e$   $\sigma$  and  $\pi$  Bonds and Lone Pairs**

parameter	$\text{VO}_3^-$ (A)	$\text{VO}_4$ (B)	$\text{VO}_4$ (C)
Atomic Charges			
$Q(\text{V})$	+1.09	+1.34	+1.33
$Q(\text{S}_{\text{Cys}})$	–0.31	–0.42	–0.42
$Q(\text{N/O}_{\text{apical}})$	–0.79 <sup>a</sup>	–0.68	–0.90
$2c-2e$ Bond Populations (el)			
V–O1 $\sigma$	1.99	1.99	1.98
V–O1 $\pi$	1.96	none	none
V–O2	1.98	1.99	1.99
V–O3	1.98	1.99	1.98
V–S	1.95	none	none
Lone Pair Populations (el)			
LP1(S)	1.94	1.94	1.94
LP2(S)	1.87	1.88	1.88
LP3(S)	none <sup>b</sup>	1.73	1.73
V–N or $\text{O}_{\text{apical}}$	none	none	none
LP1(N or $\text{O}_{\text{apical}}$ )	n/a <sup>c</sup>	1.91	1.94
LP2( $\text{O}_{\text{apical}}$ )	n/a	1.86	1.83
LP3(N or $\text{O}_{\text{apical}}$ )	1.66	1.61	1.65

<sup>a</sup>–0.79 is the atomic charge on the R<sup>60</sup> nitrogen atom in an apical position with respect to V; the total charge on the guanidinium group of this Arg is +0.6. <sup>b</sup>“none” indicates that suitable orbitals are available but not occupied. <sup>c</sup>“n/a” indicates that the LP orbitals are not present.

three complexes. There is an apparent difference between the bonding exhibited by the VHZ– $\text{VO}_3^-$  complex **A** and the other two complexes. As expected from the V–N distance of 3.2 Å,

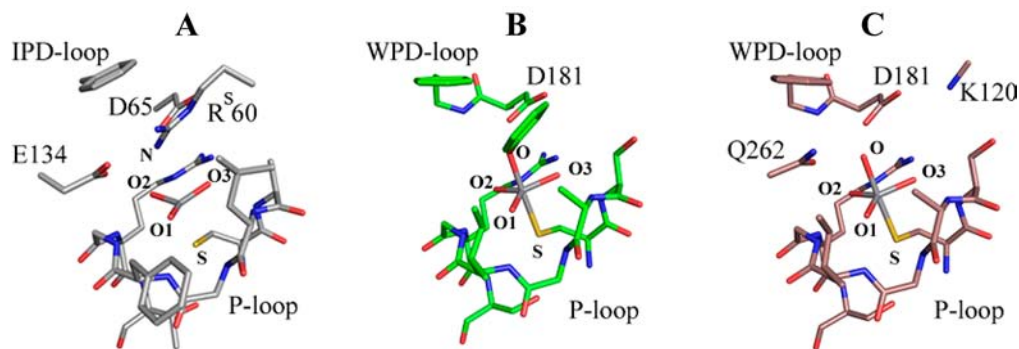


**Figure 2.** Regions of the three vanadate complexes used in the quantum-mechanical calculations: VHZ– $\text{VO}_3^-$  (**A**; PDB entry 4ERC), PTP1B–Tyr– $\text{VO}_4$  (**B**; PDB entry 3I7Z), and PTP1B– $\text{VO}_4$  (**C**; PDB entry 3I80). H atoms have been omitted for clarity. In the VHZ complex **A**, the R<sup>60</sup> residue in the active site comes from a symmetry-related VHZ molecule. DADEYL peptide has been omitted, except for the Tyr side chain.

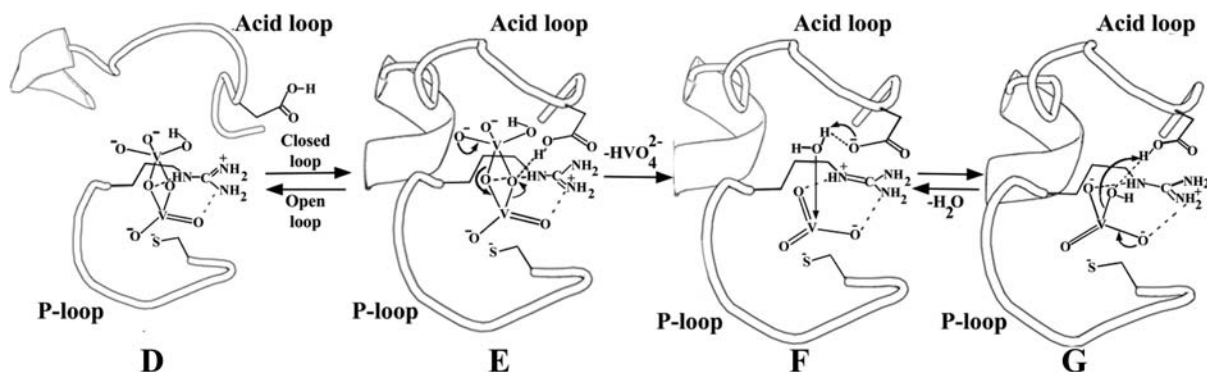


**Figure 3.** Proposed mechanism that explains the formation of a metavanadate species in the active site of VHZ. The vanadium species **D**, **F**, and **G** have been observed in crystal structures. The protonation states of the vanadium species are not known from the crystal structures but are depicted in states consistent with the pH at which the crystals were grown. **D** (PDB entry 3F9B) contains divanadate bound in the active site of the YopH W354F mutant with the catalytic WPD (acid) loop locked in a half-open conformation. **E** is a transient complex (not observed in the crystal form) showing the acid loop closure that triggers the catalytic transformation of divanadate into metavanadate; VHZ has no mobile loop, but its general acid occupies an analogous position. **F** (PDB entry 4ERC) contains metavanadate trapped in the active site of VHZ. **G** (PDB entry 3I80) contains orthovanadate in the active site of PTP1B.

there is no significant interaction between V and the apical N of R<sup>60</sup>. The partially populated lone pair (LP) on N of the distant apical Arg (1.66 |e|) donates electron density to the guanidinium group, participating in  $\pi$  resonance, and is only weakly coordinated to V through van der Waals interactions. One of the O atoms of the  $\text{VO}_3^-$  ion exhibits a  $\pi$  bond with V, representing one of the resonance structures (the lowest-energy one) possible in this  $\pi$ -delocalized  $\text{VO}_3^-$  ion. There is a clear two-center–two-electron (2c–2e) bond between V and  $\text{S}_{\text{Cys95}}$ . This bond is primarily ionic, with 79% of the electron density residing on S and 21% on V. This is consistent with the electron density gap between  $\text{S}_{\text{Cys95}}$  and V observed in the unbiased composite omit map, which is indicative of ionic rather than covalent ligand stabilization. The bonding within the vanadate moiety and its interaction with VHZ differ in several ways from those in the more conventional PTP1B complexes. In contrast to complex **A**, there is no  $\pi$  bonding within the central  $\text{VO}_3^-$  part of the ion in the PTP1B complexes **B** and **C** (Figure 2). This is reflected in different average V–O bond lengths in the X-ray structures, which are 1.70 Å for **A**, 1.89 Å for **B**, and 1.91 Å for **C**. One LP on  $\text{S}_{\text{Cys215}}$  (LP3) and one on  $\text{O}_{\text{Tyr}}$  (LP3) are populated only by ca. 1.7 |e| within the NBO localized picture. The low-populated lone pair on S (LP3) partially donates electron density to the d atomic orbitals (AOs) of V. The low-populated  $\text{O}_{\text{Tyr}}$  lone pair (LP3) primarily donates electrons into  $\pi$  resonance within the Tyr phenyl ring. However, both LP2 and LP3 on  $\text{O}_{\text{Tyr}}$  also donate to the d AOs on V.

To summarize, in the PTP1B complexes **B** and **C**, neither the V– $\text{S}_{\text{Cys}}$  nor V– $\text{O}_{\text{Tyr}}$  apical interaction is a classic 2c–2e bond. Bonding between V and these apical ligands is significant and highly delocalized among  $\text{S}_{\text{Cys}}$ , V, and  $\text{O}_{\text{Tyr}}$ . The equatorial V–O interactions are single bonds. In contrast, the VHZ– $\text{VO}_3^-$  complex **A** can be described as a  $\pi$ -delocalized  $\text{VO}_3^-$  ion with only one apical interaction, an ionic bond between V and  $\text{S}_{\text{Cys}}$ .

The complex solution chemistry of vanadate must be considered together with the chemical properties of the enzymes with which it can associate. Monomeric vanadate dominates at low concentrations, with dimeric forms becoming significant at concentrations above 0.2 mM, followed by higher oligomers.<sup>8</sup> Interconversion is rapid, and it is logical that the various forms of vanadate should be similarly labile in an enzymatic active site. There is no a priori reason that an inhibiting form of vanadate

must preform in solution before binding to the enzyme. While numerous oligomeric forms of vanadate have been documented, metavanadate in solution has not been reported, so presumably it was generated by the enzyme from some other vanadate species present in solution and subsequently stabilized by the active-site environment. We propose a simple mechanism that can explain the formation of this species from divanadate and possibly polyvanadate forms that are well-known to exist and usually dominate in solution. In light of the highly conserved nature of the active sites of PTPs, this mechanism would apply to this family as whole and potentially to any similar enzyme with a general acid. This proposal (Figure 3) incorporates the general acid conserved in PTPs and also explains why the first report of a divanadate species in the active site of a PTP was found in a YopH W354F mutant in which the flexible loop that bears the general acid is locked in a catalytically unproductive position (**D** in Figure 3).<sup>17</sup> The crystal structure of this divanadate complex shows that dimeric and possibly higher oligomeric species are capable of binding to PTPs. We believe that it is no coincidence that this complex was identified in a mutant in which general acid catalysis is disabled. Presumably, this or other dimeric forms bind to the native enzyme but are rapidly hydrolyzed to the monomer and not observed crystallographically.

According to the proposed mechanism, divanadate binds in the active site (**D** in Figure 3), and the general acid protonates one of its bridge oxygens, triggering decomposition and formation of “metavanadate”, which is stabilized by the P-loop and electrostatic interactions with the nucleophilic thiolate. The resulting complex (**F** in Figure 3) is the species trapped in the VHZ– $\text{VO}_3^-$  crystal structure. The classically observed trigonal-bipyramidal orthovanadate species can result from a process analogous to the second step of the PTP-catalyzed reaction in which a nucleophilic water attacks with positioning assistance of Q-loop residues, assuming the other apical position. Such a process would explain the high affinity and selectivity in crystal structures of PTPs for monomeric orthovanadate under conditions where oligomeric polyvanadates dominate in solution. Recent work<sup>18</sup> has shown that vanadate speciation is sensitive to surfaces such as micelles, consistent with the idea that an enzyme active site could preferentially stabilize a species such as the dimer in **D** or metavanadate in **F**.



We note that the reversible interconversion between F and G in Figure 3 provides an alternative pathway for enzyme-catalyzed metavanadate formation without invoking binding of a dimeric form. However, the VHZ crystals were grown in the presence of 10 mM vanadate, far above the 0.2 mM level at which dimeric and higher forms begin to dominate. Potent vanadate inhibition of many phosphatases across wide ranges of pH and vanadate concentration has been reported, supporting the notion that multiple forms are capable of binding and that the interconvertibility in the active site is similar to that in solution. If anything, the active site of an enzyme optimized to catalyze hydrolysis should facilitate such processes.

The metavanadate observed here is not an anomalous structure relevant only to VHZ or potentially other PTPs. A geometrically similar species has been previously observed in a crystal structure of phosphoglucomutase,<sup>19</sup> an enzyme that has no similarity to PTPs. That structure also reveals a planar  $\text{VO}_3^-$  moiety with a single apical ligand (an aspartate carboxyl group) and a similar gap in the  $2F_o - F_c$  electron density obtained from the Electron Density Server (EDS) observed at  $1.0\sigma$ .

In summary, this work shows that the interaction of vanadate with the active sites of PTPs in solution is more versatile than the simple trigonal-bipyramidal model that dominates in the PDB. The inhibitory effect of vanadate can involve dimeric and potentially higher oligomers, an important factor since such species often dominate in solution. The ability of the active-site environment to stabilize a metavanadate ion electrostatically adds another facet to the interaction of vanadate with such enzymes. In the  $\text{VHZ-VO}_3^-$  complex, there is only a single significant apical interaction, which is primarily ionic.

This complex is a good analogue of the loose metaphosphate-like transition state concluded from experimental studies. The average  $\text{V-O}_{\text{eq}}$  bond distance in the  $\text{VHZ-VO}_3^-$  structure is shorter than those in commonly observed trigonal-bipyramidal vanadate complexes but in good agreement with experimental values determined by Raman difference spectroscopy of vanadate in the active site of the related enzyme YopH.<sup>6a</sup> Hence, it is conceivable that such  $\text{VO}_3^-$  species may form more commonly than suspected in PTP-vanadate solutions, and the dominance among crystal structures of the trigonal-bipyramidal structures (e.g., B and C) arise from species that subsequently form and are more amenable to trapping. The rich speciation of vanadate in solution clearly extends to its ability to adopt multiple structures in enzyme active sites.

## ■ ASSOCIATED CONTENT

### 📄 Supporting Information

Absolute energies and atomic coordinates of the computationally analyzed structures and complete ref 16. This material is available free of charge via the Internet at <http://pubs.acs.org>.

## ■ AUTHOR INFORMATION

### Corresponding Author

[alexandrova@chem.ucla.edu](mailto:alexandrova@chem.ucla.edu); [alvan.hengge@usu.edu](mailto:alvan.hengge@usu.edu)

### Notes

The authors declare no competing financial interest.

## ■ ACKNOWLEDGMENTS

This work was supported by the NIH (Grant GM 47297 to A.C.H.) and a DARPA Young Faculty Award (N66001-11-1-4138 to A.N.A.).

## ■ REFERENCES

- (1) (a) Bishayee, A.; Waghray, A.; Patel, M. A.; Chatterjee, M. *Cancer Lett.* **2010**, *294*, 1. (b) Cam, M. C.; Brownsey, R. W.; McNeill, J. H. *Can. J. Physiol. Pharmacol.* **2000**, *78*, 829. (c) Crans, D. C.; Smees, J. J.; Gaidamauskas, E.; Yang, L. *Chem. Rev.* **2004**, *104*, 849. (d) Evangelou, A. M. *Crit. Rev. Oncol. Hematol.* **2002**, *42*, 249. (e) Heyliger, C. E.; Tahiliani, A. G.; McNeill, J. H. *Science* **1985**, *227*, 1474. (f) Rubinson, K. A. *Proc. R. Soc. London, Ser. B* **1981**, *212*, 65. (g) Tsiani, E.; Bogdanovic, E.; Sorisky, A.; Nagy, L.; Fantus, I. G. *Diabetes* **1998**, *47*, 1676. (h) Tsiani, E.; Fantusa, I. G. *Trends Endocrinol. Metab.* **1997**, *8*, 51.
- (2) (a) Crans, D. C.; Sudhakar, K.; Zamborelli, T. J. *Biochemistry* **1992**, *31*, 6812. (b) Crans, D. C.; Willging, E. M.; Butler, S. R. *J. Am. Chem. Soc.* **1989**, *112*, 427. (c) Messmore, J. M.; Raines, R. T. *J. Am. Chem. Soc.* **2000**, *122*, 9911. (d) Messmore, J. M.; Raines, R. T. *Arch. Biochem. Biophys.* **2000**, *381*, 25. (e) Stankiewicz, P. J.; Gresser, M. J. *Biochemistry* **1988**, *27*, 206.
- (3) (a) Shechter, Y. *Diabetes* **1990**, *39*, 1. (b) Bhattacharyya, S.; Tracey, A. S. *J. Inorg. Biochem.* **2001**, *85*, 9.
- (4) (a) Zhang, M.; Zhou, M.; Van Etten, R. L.; Stauffacher, C. V. *Biochemistry* **1997**, *36*, 15. (b) Brandao, T. A.; Hengge, A. C.; Johnson, S. J. *J. Biol. Chem.* **2010**, *285*, 15874. (c) Davies, D. R.; Hol, W. G. *FEBS Lett.* **2004**, *577*, 315. (d) Stankiewicz, P. J.; Tracey, A. S.; Crans, D. C. *Met. Ions Biol. Syst.* **1995**, *31*, 287. (e) Denu, J. M.; Lohse, D. L.; Vijayalakshmi, J.; Saper, M. A.; Dixon, J. E. *Proc. Natl. Acad. Sci. U.S.A.* **1996**, *93*, 2493.
- (5) (a) Lassila, J. K.; Zalatan, J. G.; Herschlag, D. *Annu. Rev. Biochem.* **2011**, *80*, 669. (b) Hengge, A. C. *Adv. Phys. Org. Chem.* **2005**, *40*, 49. (c) Hengge, A. C.; Zhao, Y.; Wu, L.; Zhang, Z. Y. *Biochemistry* **1997**, *36*, 7928. (d) Hengge, A. C.; Sowa, G. A.; Wu, L.; Zhang, Z. Y. *Biochemistry* **1995**, *34*, 13982.
- (6) (a) Krauss, M.; Basch, H. *J. Am. Chem. Soc.* **1992**, *114*, 3630. (b) Deng, H. C. R.; Huang, Z.; Zhang, Z. Y. *Biochemistry* **2002**, *41*, 5865.
- (7) Crans, D. C.; Bunch, R. L.; Theisen, L. A. *J. Am. Chem. Soc.* **1989**, *111*, 7597.
- (8) Crans, D. C.; Rithner, C. D.; Theisen, L. A. *J. Am. Chem. Soc.* **1990**, *112*, 2901.
- (9) Alonso, A.; Burkhalter, S.; Sasin, J.; Tautz, L.; Bogetz, J.; Huynh, H.; Bremer, M. C.; Holsinger, L. J.; Godzik, A.; Mustelin, T. *J. Biol. Chem.* **2004**, *279*, 35768.
- (10) Pannifer, A. D.; Flint, A. J.; Tonks, N. K.; Barford, D. *J. Biol. Chem.* **1998**, *273*, 10454.
- (11) Pettersen, E. F.; Goddard, T. D.; Huang, C. C.; Couch, G. S.; Greenblatt, D. M.; Meng, E. C.; Ferrin, T. E. *J. Comput. Chem.* **2004**, *25*, 1605.
- (12) Denu, J. M.; Dixon, J. E. *Proc. Natl. Acad. Sci. U.S.A.* **1995**, *92*, 5910.
- (13) (a) Carpenter, J. E.; Weinhold, F. *THEOCHEM* **1988**, *169*, 41. (b) Foster, J. P.; Weinhold, F. *J. Am. Chem. Soc.* **1980**, *102*, 7211. (c) Reed, A. E.; Weinhold, F. *J. Chem. Phys.* **1983**, *78*, 4066. (d) Reed, A. E.; Curtiss, L. A.; Weinhold, F. *Chem. Rev.* **1988**, *88*, 899.
- (14) (a) Parr, R. G.; Yang, W. *Density-Functional Theory of Atoms and Molecules*; Oxford University Press: Oxford, U.K., 1989. (b) Becke, A. D. *J. Chem. Phys.* **1993**, *98*, 5648. (c) Perdew, J. P.; Chevary, J. A.; Vosko, S. H.; Jackson, K. A.; Pederson, M. R.; Singh, D. J.; Fiolhais, C. *Phys. Rev. B* **1992**, *46*, 6671.
- (15) (a) Clark, T.; Chandrasekhar, J.; Spitznagel, C. W.; Schleyer, P. v. R. *J. Comput. Chem.* **1983**, *4*, 294. (b) Frisch, M. J.; Pople, J. A.; Binkley, J. S. *J. Chem. Phys.* **1984**, *80*, 3265.
- (16) Frisch, M. J.; et al. *Gaussian 09*, revision A; Gaussian, Inc.: Wallingford, CT, 2009.
- (17) Brandao, T. A.; Robinson, H.; Johnson, S. J.; Hengge, A. C. *J. Am. Chem. Soc.* **2009**, *131*, 778.
- (18) Crans, D. C.; Baruah, B.; Ross, A.; Levinger, N. E. *Coord. Chem. Rev.* **2009**, *253*, 2178.
- (19) Lu, Z.; Dunaway-Mariano, D.; Allen, K. N. *Proc. Natl. Acad. Sci. U.S.A.* **2008**, *105*, 5687.